비선형 내점법을 이용한 전력계통 평형점 최적화 (EOPT)

송화창 호세 로델 도사노
국립군산대학교 전자정보공학부

Power System Equilibrium Optimization (EOPT) with a Nonlinear Interior Point Method

Hwachang Song Jose Rodel Dosano
Kunsan National University

Abstract - This paper presents a new methodology to calculate an optimal solution of equilibrium to power system differential algebraic equations. It employs a nonlinear interior point method for solving the optimization formulation, which includes dynamic equations representing two-axis synchronous generator models with AVR and speed governing control, algebraic equations, and steady-state nonlinear loads. Equilibrium optimization (EOPT) is useful for diverse purposes in power system analysis and control with consideration of the system frequency constraint.

1. Introduction

Power systems should be operated within a region of security, which is constrained by both operation and security limits [1]. In the early 1960's, the concept of optimal power flow (OPF) was introduced [2], which pursues economic dispatch solving the power flow equations. This tool can also be useful for correction of static security for the systems in contingent states [2-4]. However, power systems can be modeled with a set of differential-algebraic equations (DAEs) [5], assuming that electromagnetic transients are decomposed out. There naturally exists difference of the results depending on whether or not it considers dynamic aspects, even when focusing on system equilibrium.

This paper presents a new methodology to determine an optimal solution of equilibrium to power systems'DAEs. The formulation of equilibrium optimization (EOPT) contains dynamics of the two-axis generator model, automatic voltage regulation and simple speed governing control, and includes the network equations and static nonlinear loads. To solve the formulation, in this paper, a nonlinear interior point method (NIPM) is employed, which a Newton-type method with log-barrier penalty functions for coping with the inequality constraints. In EOPT, the system frequency constraint can be included, so using EOPT, controls satisfying the acceptable frequency change can be obtained with a certain objective function. In case study, two examples of active and reactive power dispatch are given with a 6-bus test system to show the usefulness of EOPT.

2. EOPT Formulation and Solution Technique

The EOPT formulation can be expressed in a brief form as follows:

$$\begin{aligned} \min \quad & f(x,y,u,p) \\ s.t. \quad & h_D(x,y,u,p)=0 \\ & h_A(x,y,u,p)=0 \\ & g_{\min} \le g(x,y,u,p) \le g_{\max} \end{aligned} \tag{1}$$

where x, y, u and p denote the vectors for state, algebraic, contr ol variables and parameters, respectively. In (1), $f(\cdot)$ represents re present the objective function. $h_D(\cdot)$ and $h_A(\cdot)$ stand for the functi on vector of the equality constraints for differential equations and algebraic equations, respectively. $g(\cdot)$ is the inequality function ve ctor for operational and parametric limits, and $g_{\max}$ and $g_{\min}$ are t he upper and lower limits of $g(\cdot)$ respectively.

The difference of (1) from the formulation of the conventional OPF is inclusion of the equilibrium equations for dynamic models ($h_D(\cdot)$=0). For synchronous machines, this paper makes use of the dynamic models in [6] in EOPT implementation, and they include the two-axis synchronous generator model with AVR and speed governing control. For load representation, active and reactive loa ds at bus i, P_{li} and Q_{li}, are modeled as follows:

$$P_{li} = P_{lio}(V_i / V_{io})^{\alpha i} \tag{2.a}$$

$$Q_{li} = Q_{lio}(V_i / V_{io})^{\beta i} \tag{2.b}$$

where P_{lio} and Q_{lio} denote active and reactive power load at the nominal voltage V_{io}, α_i and β_i are the constants for voltage dependency of the active and reactive load.

EOPT incorporates the following objective function:

$$f(\cdot) = \sum_{i\in SG} w_{Pgsi}(P_{gsi} - P_{gsi}^0)^2 + \sum_{i\in SG} w_{Vrefi}(V_{refi} - V_{refi}^0)^2 \tag{3}$$

where S_G indicates the set of generators in the system, and w_{Pgsi} and w_{Vrefi} denote weighting factors for control of P_{gsi} and V_{refi}. These two are designated real power generation and reference voltage of AVR of generator i. The superscript 0 represents the initial value of each control variable.

EOPT solves the optimum of (1) with a nonlinear interior point method (NIPM). NIPM is one of Newton-type methods, which finds a solution satisfying the *Karush-Kuhn-Tuker* (KKT) first-order optimality necessary condition. NIPM first introduces slack variables (≥0) to make inequality constraints to equality ones; then, it establishes the Lagrange function which includes the objective function, the functions of the total equality constraints, and a scalar log barrier function of the slack variables. For (1), the Lagrange function can be expressed as follows:

$$\begin{aligned} L(z,s_L,s_U,\lambda_D,\lambda_A,\pi_L,\pi_U;\mu) = f(z) \\ -\lambda_D^T \cdot h_D(z) - \lambda_A^T \cdot h_A(z) \\ -\pi_L^T(g(z) - s_L - g_{\min}) \\ -\pi_U^T(g(z) + s_U - g_{\max}) \\ -\mu(\sum_i \ln s_{Li} + \sum_i \ln s_{Ui}) \end{aligned} \tag{4}$$

where the following notations are made:
z: the state vector (=[x y u p]^T in (1)),
s_L: the lower slack variables vector for the lower limits of $g(\cdot)$,
s_U: the upper slack variables vector for the upper limits of $g(\cdot)$,
λ_D: Lagrangian multipliers vector for $h_D(\cdot)$=0,
λ_A: Lagrangian multipliers vector for $h_A(\cdot)$=0,
π_L: Lagrangian multipliers vector for $g(\cdot)-s_L-g_{\min}$=0,
π_U: Lagrangian multipliers vector for $g(\cdot)-s_U-g_{\max}$=0,
μ: barrier parameter.

The procedure of NIPM for solving the optimum is outlined as follows:

Step 1: Initialize the primal and dual variables.

Step 2: Compute the complementary gap, G_C, and power flow residuals. If the gap and the residuals are less than the given tolerances, stop.

$$G_C = \pi_L^T s_L + \pi_U^T s_L$$

Step 3: Set the barrier parameter with the following equation:

$$\mu = c\frac{G_C}{2n_C}$$

where n_C is the number of constraints and c (0<c<1) is the centering parameter introduced in [7].

Step 4: Construct the linear system in (7) and solve the correcti on vector. With (6), obtain s_L, s_U, π_L, and π_U.

Step 5: Determine primal and dual step length without linearly violating the constraints.

Step 6: Update the primary and dual variables and go to Step 2.

3. Numerical Results

This section describes an example demonstrating the usefulness of EOPT with 6-bus test-system. Fig. 2 shows the one-line diagram of the system with line reactance data. Table I and II shows the load flow data of the base case and generator data in use, respectively.

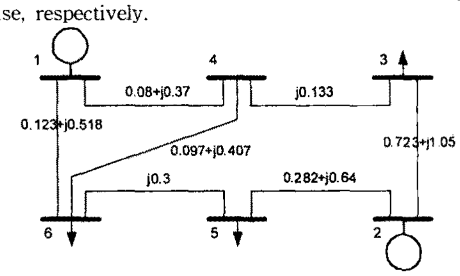

<Fig. 1> One-line diagram of 6-bus test system

<Table I> Load flow data of the base case

Bus #	Volt [pu]	Angle [degree]	P_L [MW]	Q_L [MVAr]	P_G [MW]	Q_G [MVAr]
1	1.0500	0.00	·	·	96.98	62.39
2	1.0000	-0.42	·	·	50.00	7.43
3	0.9510	-13.27	55.00	13.00	·	·
4	0.8926	-9.98	·	·	·	·
5	0.8478	-12.52	30.00	18.00	·	·
6	0.8753	-12.43	50.00	5.00	·	·

<Table II> Generator data of the system

Gen #	Xd	Xq	Xd'	Xq'	Rs	Tdo'	Tqo'
1	0.995	0.568	0.195	0.568	0	10.8	0.5
2	0.619	0.134	0.238	0.365	0	7.4	0.5
	D	H	MVA	Ke	Te	Se	Ka
1	0	6.41	200	1	0.25	0.1	20
2	0	3.8	113	1	0.25	0.1	20
	Ta	Kf	Tf	Tch	Tg	Rg	Vrmax
1	0.06	0.04	1	1.6	0.2	0.05	3
2	0.06	0.04	1	1.6	0.2	0.05	3

3.1 Reactive power dispatch with V_{ref}

As seen in Table I, voltage magnitudes of bus 4, 5, and 6 are below 0.9 [pu], so this study first performs reactive power dispatch of the two generators using control of V_{ref} to enhance voltage profile such that all the bus voltages are within the range of 0.9-1.1. For this purpose, weighting factors of $w_{P_{gsi}}$s are set to 0, and $w_{V_{refi}}$s to 100. Table III shows other settings of parameters associated with the objective function. From Table III, one can notice that V_{ref} of each generator is the main control measure, and that each P_{gs} is able to slightly change within the corresponding range. The role of P_{gs} is closely related to system frequency in equilibrium, and in this simulation, the used the upper and lower limits of per-unit system frequency are 0.999 and 1.001.

<Table III> Parameter setting in reactive power dispatch

Gen. #	P_{gs}^0	P_{gs}^{min}	P_{gs}^{max}	V_{ref}^0	V_{ref}^{min}	V_{ref}^{max}
1	0.9698	0.9598	0.9798	1.127693	1.0	1.2
2	0.5000	0.4900	0.5100	1.058023	1.0	1.2

The simulation takes 11-iterations to obtain the optimal solution that satisfies the stopping rule with thetolerance of the complementary gap and the maximum mismatch in equality constraint. They are set to 10-5 and 10-4, respectively. EOPT provides the optimal setting of Vref for generator 1 and 2, they are 1.16671285 [pu] and 1.1023135 [pu], respectively. Table IV shows the status of network variables after the simulation. The system voltage profile is improved, so active power generation is slightly reduced, and the voltage constraint of bus 5 is bounded. From Table IV, one can notice that voltage angle of bus 1, which was the slack bus in Table I, is now changed to -1.74 [degree]. The reason is that in EOPT the reference angle is the rotor angle of bus 2. The per-unit system frequency after EOPT execution is 1.0004988, which is within the designated limit

3.2 Active power dispatch with P_{gs}

In the second simulation, active power dispatch using P_{gs} is performed. Table V shows the setting of the objective function related parameters for this simulation. Table VI describes the limits of active power flows of three selected lines and their initial values. These limits provide the reason of active power dispatch. This simulation applies the same range for per-unit system frequency, 0.999 - 1.001.

Using the same stopping rule as in reactive power dispatch, the simulation takes 12-iteration to obtain the solution, and it is within the active power flow constraints. The binding constraint is the per-unit system frequency limit. Table VII shows the network variables at the solution. Reactive power generation at each generator is not that changed, compared to the result in Table VI, but active power generation is much more re-dispatched. At the solution, the rotor angle of generator 1 is -0.31745489 [degree] and that of generator 2 is 0.1202430 [degree].

<Table IV> Network variables after EOPT-reacitve power dispatch

Bus #	Volt [pu]	Angle [degree]	P_L [MW]	Q_L [MVAr]	P_G [MW]	Q_G [MVAr]
1	1.0907	-1.74	·	·	96.98	50.36
2	1.0411	-0.03	·	·	48.07	11.51
3	0.9390	-10.77	55.00	13.00	·	·
4	0.9633	-7.42	·	·	·	·
5	0.9000	-10.13	30.00	18.00	·	·
6	0.9426	-9.72	50.00	5.00	·	·

<Table V> Parameter setting in active power dispatch

Gen. #	P_{gs}^0	P_{gs}^{min}	P_{gs}^{max}	V_{ref}^0	V_{ref}^{min}	V_{ref}^{max}
1	0.9698	0.6000	1.5000	1.127693	1.166	1.168
2	0.5000	0.3000	1.0000	1.058023	1.102	1.104

<Table VI> Active power flow limits of the three selected lines and their intial flow

Line	Fmin [MW]	Fmax [MW]	Flow [MW]
1 - 4	-40	40	50.8
1 - 6	-40	40	44.5
2 - 5	-50	50	31.9

<Table VII> Network variables after EOPT-active power dispatch

Bus #	Volt [pu]	Angle [degree]	P_L [MW]	Q_L [MVAr]	P_G [MW]	Q_G [MVAr]
1	1.0901	-14.47	·	·	73.05	60.12
2	1.0406	-2.68	·	·	78.82	12.20
3	0.9089	-23.64	55.00	13.00	·	·
4	0.9456	-20.93	·	·	·	·
5	0.8612	-20.02	30.00	18.00	·	·
6	0.9266	-22.50	50.00	5.00	·	·

4. Conclusions

This paper presents a methodology to calculate an optimal solution of equilibrium to power system differential algebraic equations. The formulation of EOPT incorporates the equality constraints, equilibrium equations of dynamic models and the network equations. To solve it, EOPT employs a nonlinear interior point method. In case study, this paper shows illustrative examples of active and reactive dispatch directly using control of the designated real power generation, P_{gs}, and AVR reference voltage, V_{ref} in dynamic models. EOPT can provide control strategies with consideration of the system frequency constraint.

[References]

[1] B. Stott, O. Alsac, and A. J. Monticelli, "Security analysis and optimization," Proc. of IEEE, vol. 75, pp. 1623-1644, Dec. 1987.

[2] J. Carpentier, "Contribution to the economic dispatch problem,"Bull. Soc. France Elect., vol. 8, pp. 431-437.

[3] H. W. Dommel and W. Tinney, "Optimal power flow solutions," IEEE Trans. on PAS, vol. 87, pp. 1866-1876, 1968.

[4] D. I. Sun, B. Ashley, B. Brewer, B. A. Hughes, and W. F. Tinney, "Optimal power flow by Newton approach," IEEE Trans. on PAS, vol. 103, no. 10, pp. 2864-75, Oct. 1984.

[5] P. Kundur, Power System Stability and Control, McGraw-Hill, 1994.

[6] Y. Zhou and V. Ajjarapu, "Local parameterization based tracing for stability boundary, optimal margin control and time domain simulation," presented at Bulk Power System and Control V, Aug. 26-31, 2001, Onomichi, Japan.

[7] H. Wei, H. Sasaki, J. Kubokawa and R. Yokoyama, "An interior point nonlinear programming for optimal power flow problems with a novel data structure," IEEE Trans. on Power Systems, vol. 13, no. 3, pp. 870-877, Aug. 1998.